MQXFB assembly

S. Izquierdo Bermudez and Penelope Quassolo on behalf of the MQXF team

Acknowledgements: Stephane Triquet, Nicholas Lusa, Attilio Milanese, Juan Carlos Perez, Ezio Todesco, Arnaud Devred and all the MQXFB/A teams.

Acknowledgments

- US HL-LHC Accelerator Upgrade Project (AUP)
  - BNL: K. Amm, M. Anerella, A. Ben Yahia, H. Hocker, P. Joshi, J. Muratore, J. Schmalzle, H. Song, P. Wanderer
  - FNAL: G. Ambrosio, G. Apollinari, M. Baldini, J. Blowers, R. Bossert, R. Carcagno, G. Chlachidze, J. DiMarco, S. Feher, S. Krave, V. Lombardo, C. Narug, A. Nobrega, V. Marinozzi, C. Orozco, T. Page M. Parker, S. Stoynev, T. Strauss, M. Turenne, D. Turrioni, A. Vouris, M. Yu
  - LBNL: D. Cheng, P. Ferracin, J. Ferradas Troitino, L. Garcia Fajardo, E. Lee, M. Marchevsky, M. Naus, H. Pan, I. Pong, S. Prestemon, K. Ray, G. Sabbi, G. Vallone, X. Wang
  - NHFML: L. Cooley, J. Levitan, J. Lu, R. Walsh
- CERN
  - G. Arnau Izquierdo, J. Axensalva, A. Ballarino, M. Bajko, T.A. Bampton, C. Barth, S.T. Becle, R. Berthet, N. Bourcey, B. Bordini, T. Boutboul, A. Cherif, M. Crouvizier, A. Devred, N. Eyraud, L. Favier, L. Fiscarelli, J. Fleiter, K. Kandemir, M. Guinchard, L. Grand-Clement, O. Housiaux, S. Izquierdo Bermudez, S. Luzieux, F. Mangiarotti, A. Milanese, A. Moros, P. Moyret, S. Mugnier, C. Petrone, J.C. Perez, D. Perini, M. Pozzobon, H. Prin, R. Principe, D. Pugnat, K. Puthran, P.M. Quassolo, E. Ravaioli, J.P. Rigaud, P. Rogacki, S. Russenschuck, T. Sahner, S. Sgobba, S. Straarup, E. Todesco, S. Triquet, A. Vieitez Suarez, G. Willering

What is new from last CM?

- Three magnets assembled last year, all following the new assembly procedure with auxiliary bladders in the cooling hole channels,

MQXFBMT4
October-November 2023

MQXFB03
April-May 2023

MQXFB04
Sept-October 2023

Outline

- Magnets overview
- Lessons learnt
- Overview on assembly data
- Conclusion

Outline

- **Magnets overview**
- Lessons learnt
- Overview on assembly data
- Conclusion

MQXFBMT4

- ***Coils:***
  - 104, 105 and 107: non-limiting coils from BP1, very early-stage production (2017-2018)
  - 127: first ‘transition coil’, minor modifications with respect to previous coils (larger gaps between poles, rounded edges..). Same observables (hump & belly) as the coils assembled in previous magnets (BP1-BP2-BP3-B02)

- ***Goal:***
  - Improve our understanding on the phenomenology for conductor limitation, in case MQXFB03 coils do not reach performance (*unknowns-unknowns*) and we need to go back to the ‘old’ coil fabrication process
  - Practice coil replacement. We follow AUP strategy for the shimming, based on the virgin coil geometry measurements (and not after cold powering test)

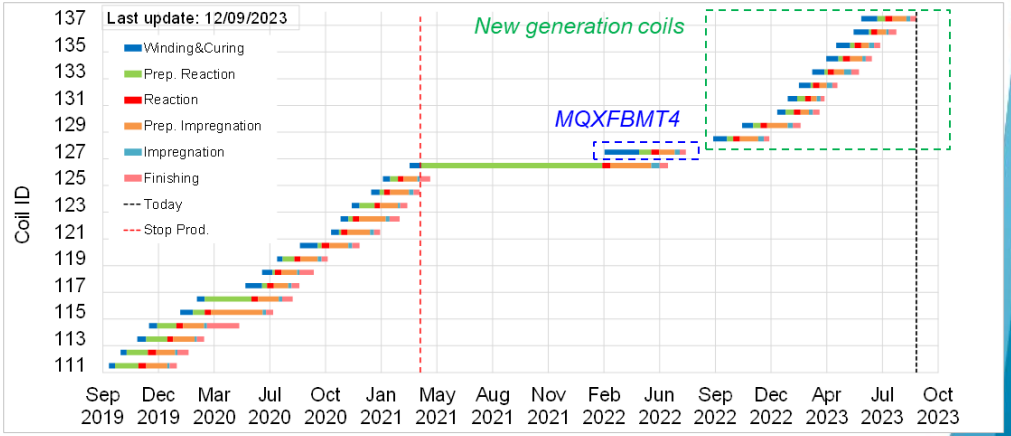

MQXFB03

- ***Coils:***
  - 128-129-130-131, the four first ‘New Generation’ coils (more info here)
- ***Difference with respect to MQXFB02***: coil geometry
  - MQXFB03 coils are smaller than nominal, with no-belly
  - MQXFB03 coils have a mid-plane angular deviation (the coil covers 89.6 degrees instead of 90 degrees)

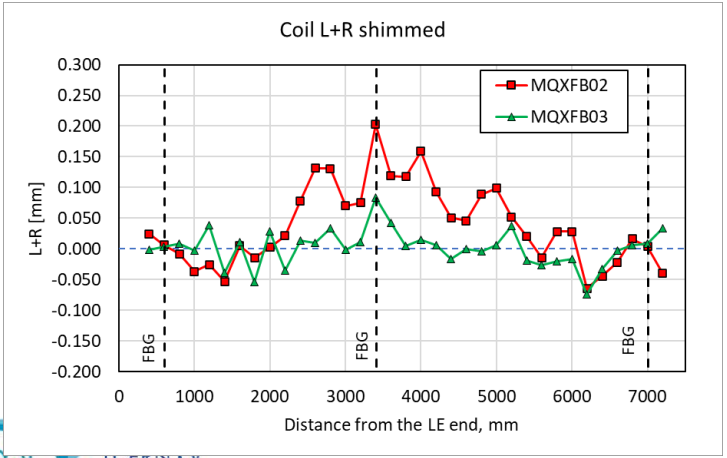

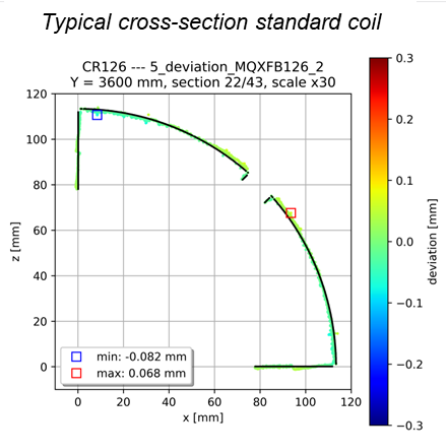

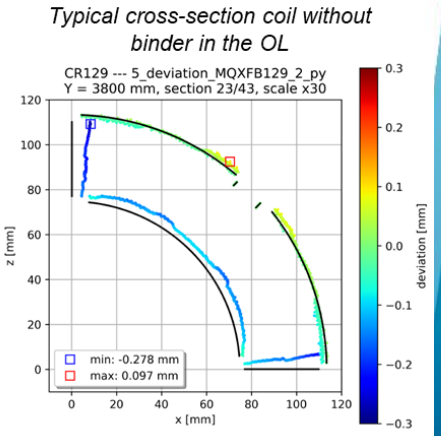

Assessment of the ‘new coil geometry’ impact

- Under conservative assumptions, according to FEM, the 0.2 deg angular deviation corresponds to an increase of ≈ 15 MPa increase in the mid-plane stress (inner edge) under conservative assumptions according to FEM

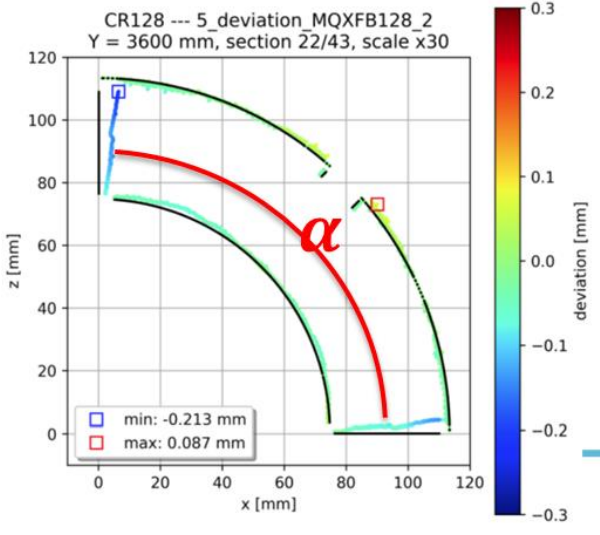

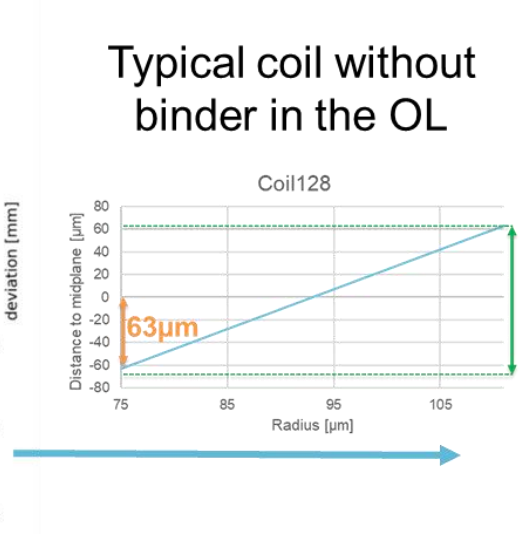

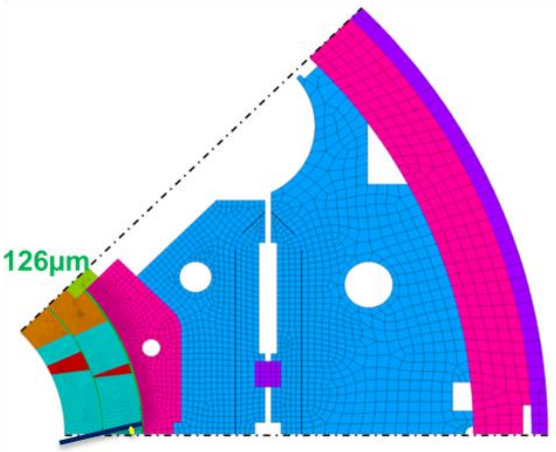

[Indico 1259143]

Assessment of the ‘new coil geometry’ impact

- With the objective of better assessing the impact of the “new” coil geometry on the contact pressure between coils (mid-planes), we explored the use of a mock-up for compressive coil tests

- Optimization of the test setup using a simplified 3D FE model. Contacts between the form-block and baseplate are open (checked with filler gauges)

- All components have been measured using the FARO arm for the detailed preparation of the required shimming
  - Torque applied = 250 Nm
  - Target σ_{avg} (mid-plane) ~ 12 MPa

- Difference in pressure distribution with the two geometries is minor, at the 10 MPa level or below

Based on these results, the difference in coil geometry is not compensated during assembly, and we target MQXFB02 pre-load level

Setup: Indico 1259143
Results: Indico 1262277

Assessment of the ‘new coil recipe’ impact

- The ceramic binder has an impact on the mechanical strength of the S2-glass braided insulation → does it have an impact on the mechanical properties of the impregnated coil?
- In parallel, a mechanical characterization on coil and ten-stack samples was launched.
  - First measurements on coils show a large impact on thermal contraction in the azimuthal direction (4 mm/m wo binder vs 2.3-2.8 mm/m w. binder
  - Measurements on ten stacks show a much smaller impact (2.8 mm/m vs 2.4 mm/m)

EN-MME

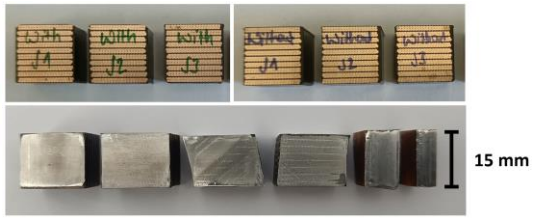

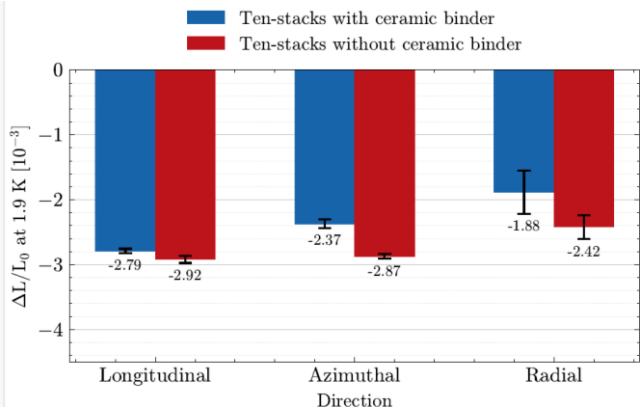

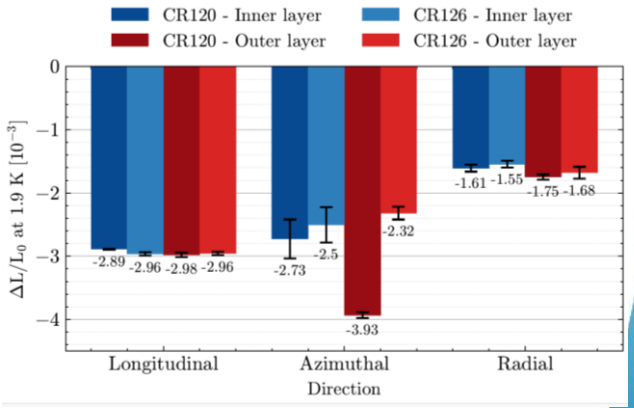

See S.Holl, Study on the thermal contraction behavior of state-of-the-art Nb_3Sn superconducting magnet coils in the longitudinal, azimuthal, and radial direction, submitted for publication, submitted for publication

MQXFB04

- ***Coils:*** 132-133-134-135, the next four ‘New Generation’ coils (more info here)
- ***Goal:*** repeat MQXFB03

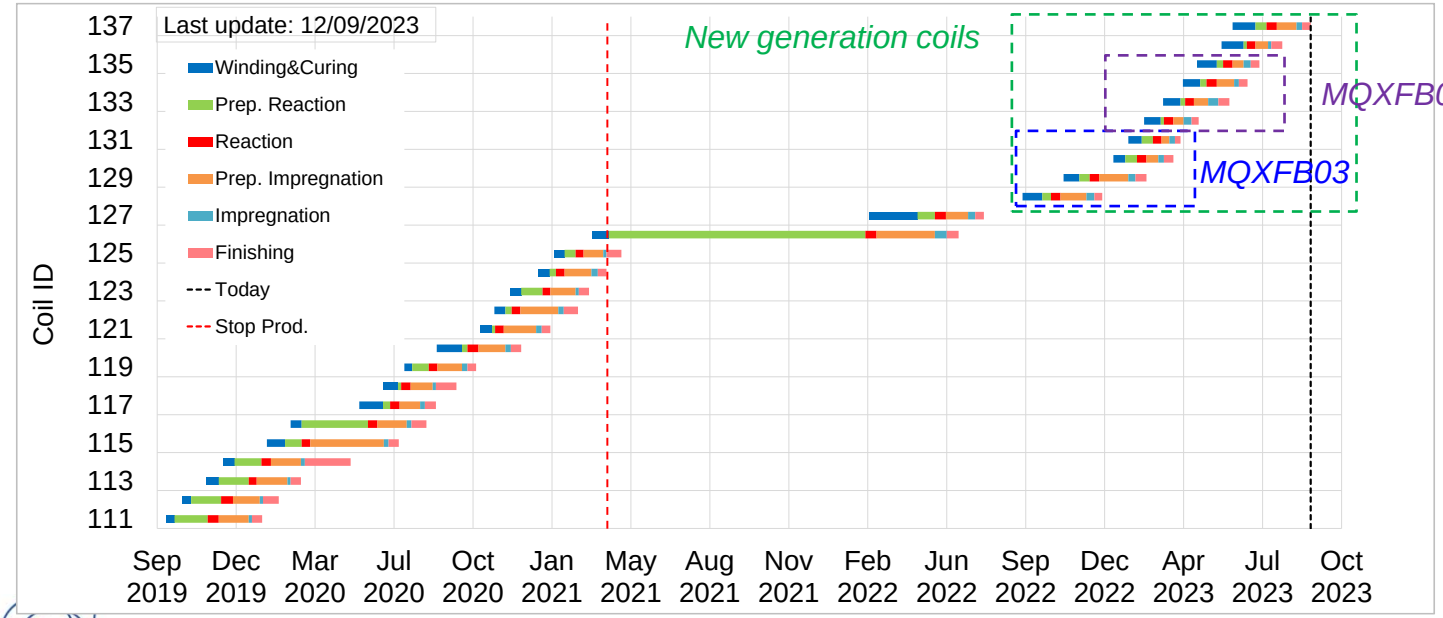

Outline

- Magnets overview
- **Lessons learnt**
- Overview on assembly data
- Conclusion

Bladder failure

- Bladder failure in MQXFBMT4 (EDMS 2803022):

Failure mode indicates that the bladder was out of the masters (not supported). Positioning was checked before starting the loading. A second bladder was replaced preventively for the same reason.

Like MQXFBP1, MQXFBMT2 → FBG strain drift after failure. https://indico.fnal.gov/event/57918/

Bladder failure in MQXFBMT4

Improved layout from MQXFBMT4

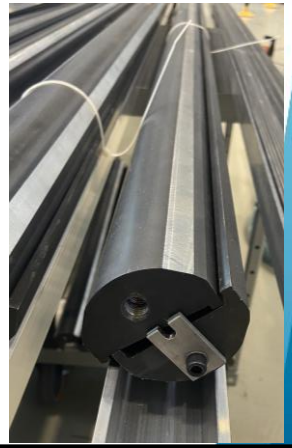

Other minor improvements

- Ground insulation forming tool optimized to host smaller coils
- Coil bumpers modified to host a cold bore tube with 0.5 mm insulation
- Iteration on the end-plate alignment tooling
- Master geometrical control before assembly

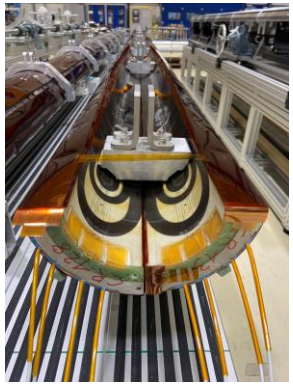

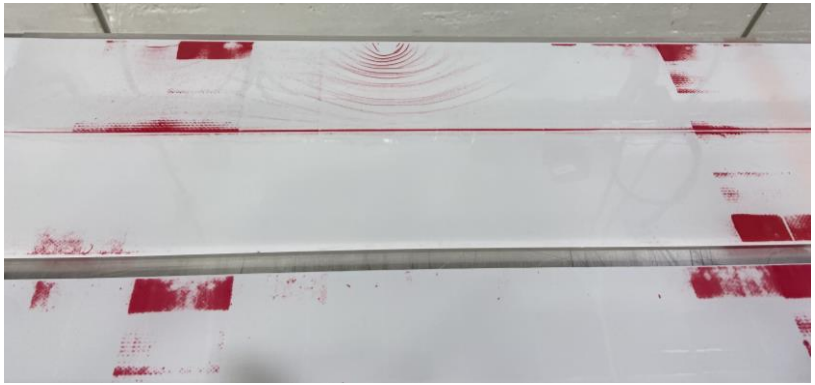

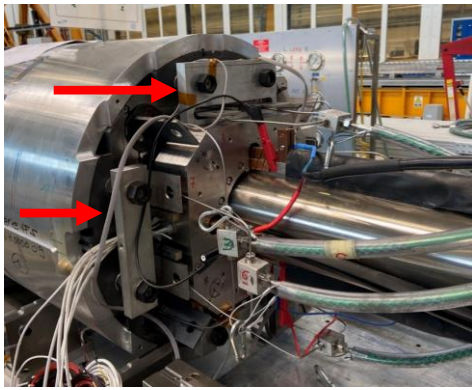

- For a more exhaustive list, see https://indico.cern.ch/event/1327153/ and https://indico.cern.ch/event/1269409

Outline

- Magnets overview
- Lessons learnt
- **Overview on assembly data**
- Conclusion

Yoke-shell modules

- Monitored parameters:
  - Shell strain
  - Bladder pressure
  - Yoke cavity size, defined as the average of the horizontal (DH1 + DH2)/2 or the vertical (DV1 + DV2)/2 dimensions
  - Yoke uniformity, defied as the average of the vertical or horizontal cavity dimension in each cross-section with respect to the measured average vertical or horizontal dimension of the entire yoke shell module
  - Yoke squareness, defied as the difference between the left and right (DV1 – DV2) or top and bottom (DH1 – DH2) dimensions

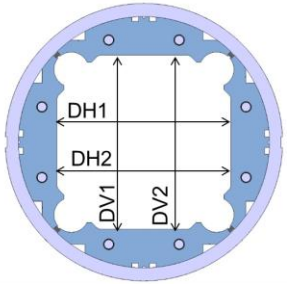

Yoke cavity size (vertical sub-assembly)

- Yoke cavity size within targets
  - **The average vertical and horizontal yoke cavity dimensions** at each cross-section **shall be within +385.125 -0.125/+0.275 mm along the module length.**

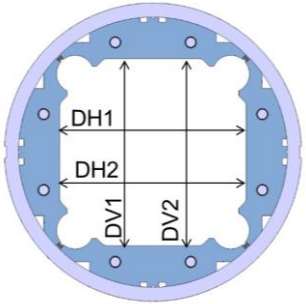

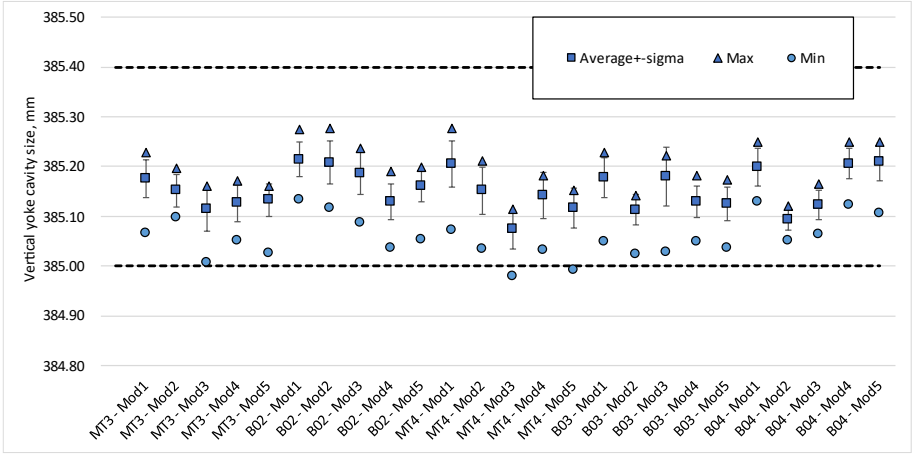

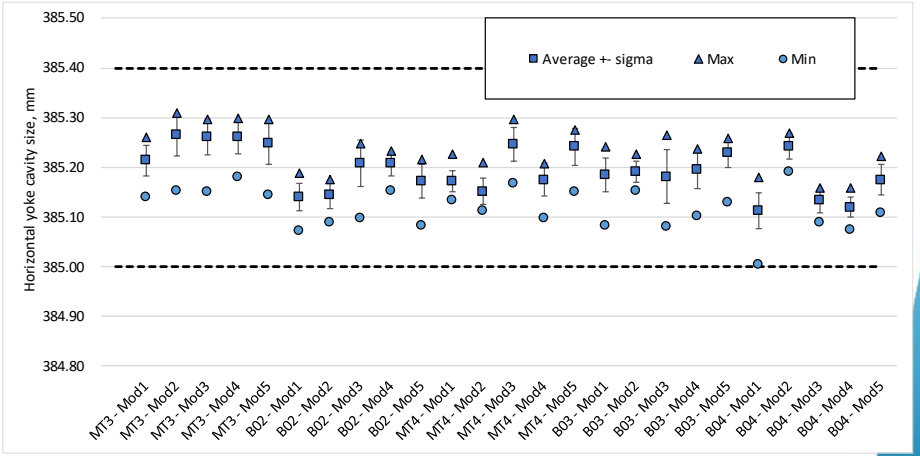

Yoke cavity size (vertical sub-assembly)

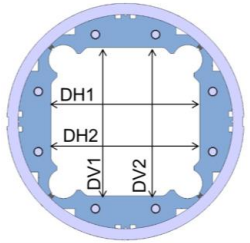

- Squareness and uniformity
  - **The average vertical and horizontal uniformity** at each cross-section **shall be within -0.15/+0.15 mm.**
  - **The average vertical and horizontal squareness** at each cross-section **shall be within -0.10/+0.10 mm.**

Squareness

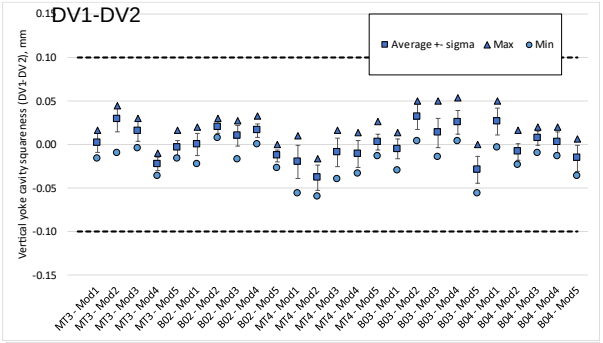

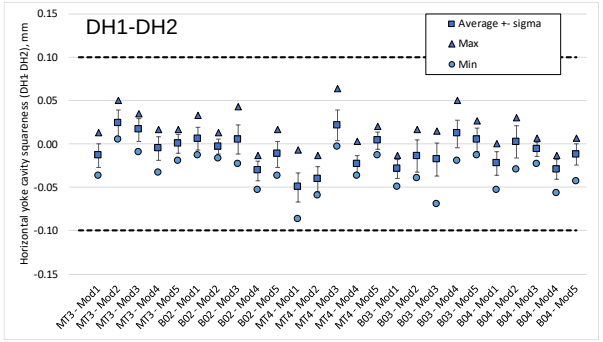

Uniformity

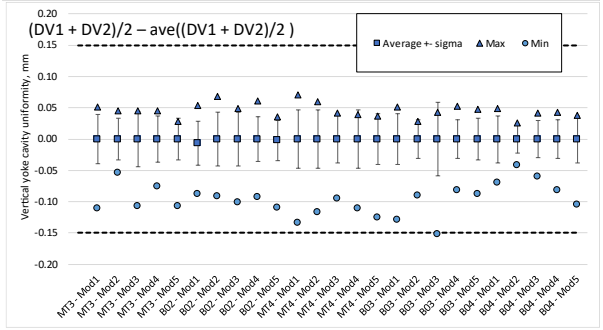

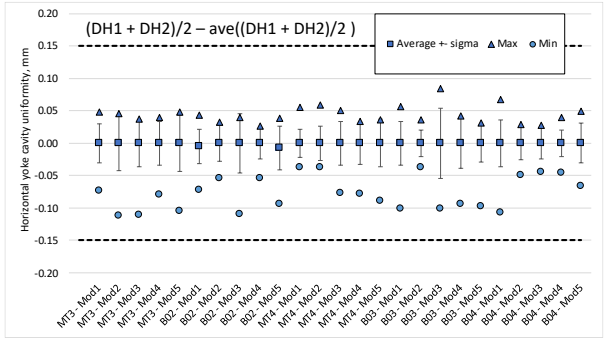

Vertical yoke-shell sub-assembly

- Strain and bladder pressure within targets
  - Yoke keys were 12.1 mm thick in all the cases below

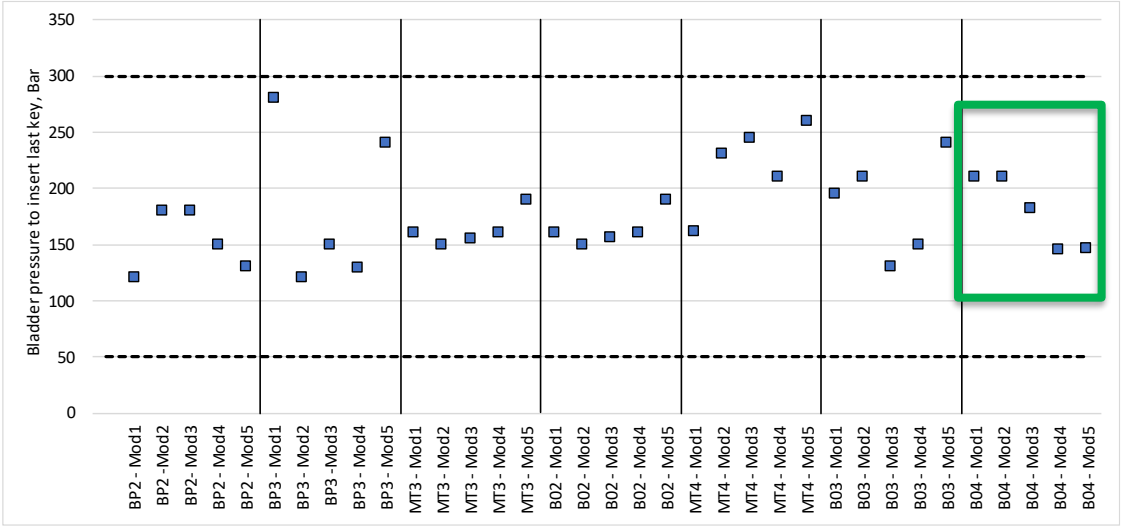

Horizontal yoke-shell assembly

- **The average developed length in the middle of each shell shall be 1929.4 -0.2/+0.3 mm.**
  - The developed length in relax state is $1928.9^{-0/+0.3}$ mm and the increase of circumference for 12.1 mm yoke key is 0.4 mm.
- **The minimum average gap between aluminium shells of adjacent modules shall be 0.2 mm**
- Yoke cavity is measured again once the modules are assembled, and shall be consistent with the vertical yoke-shell subassembly measurements
- The total length of the structure shall be 7521 ± 5 mm

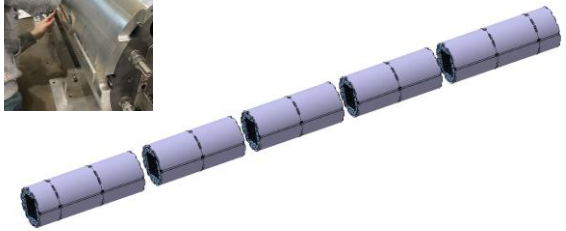

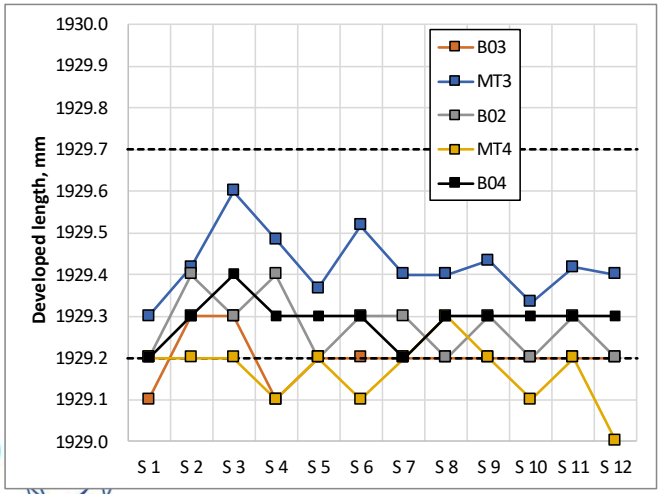

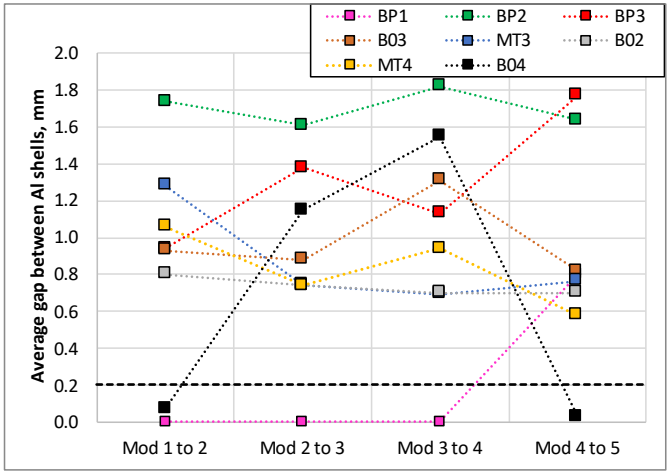

Coil pack radial size

- **The gap between collars and insulated coils with respect to the nominal dimension, considering for each z location the average among the four coils, shall be -0.125 mm -0.125 / +0.075 mm.**

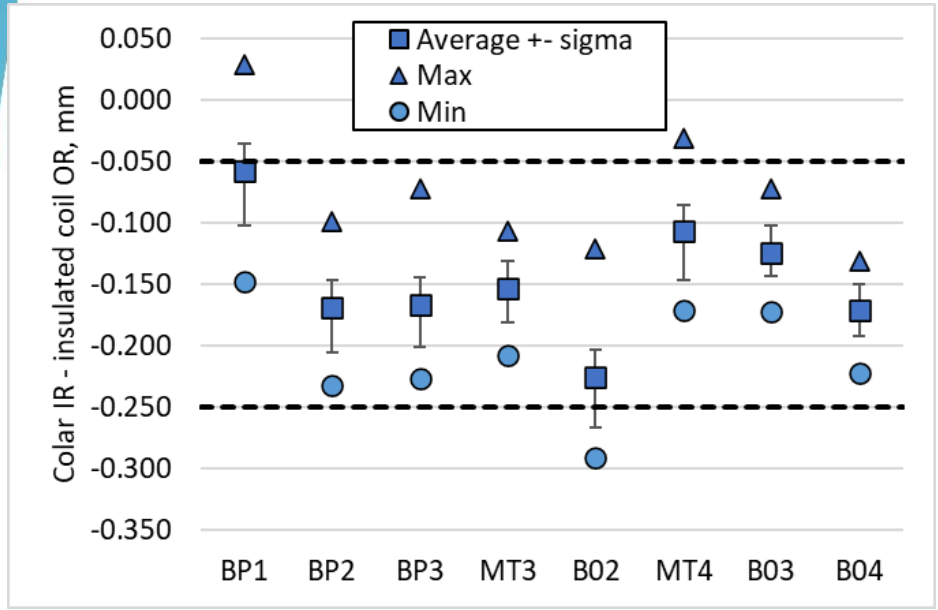

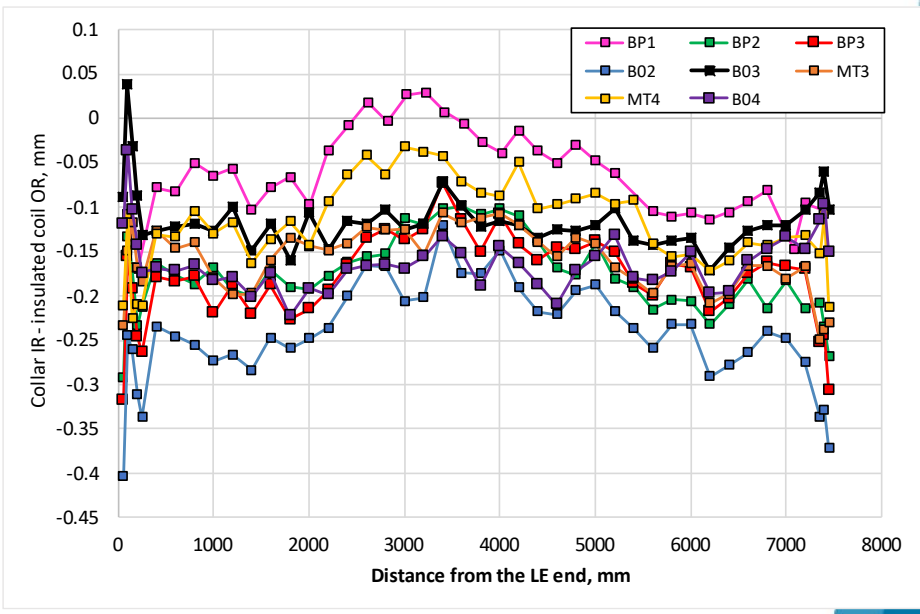

Pole-key gap

- **The average pole key gap (per side) along the magnet length shall be +0.400 ±0.100 mm in each quadrant.**
- **The minimum pole key gap (per side) in any quadrant and in any longitudinal location shall be > +0.300 mm.**
  - From MQXFB02, pole keys are machined removing 250 µm on each side from the original key (lessons learnt from A07&A08)
  - We have a more uniform pole key gap along the length than in previous assemblies (no coil belly)

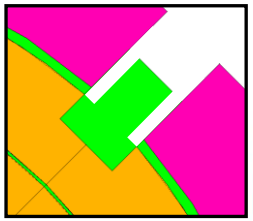

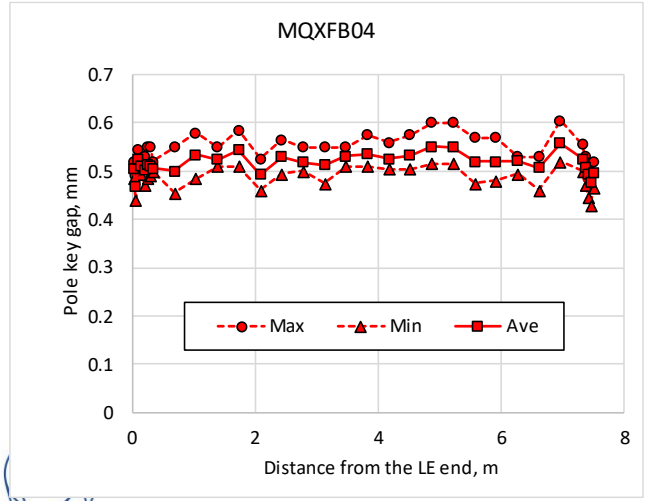

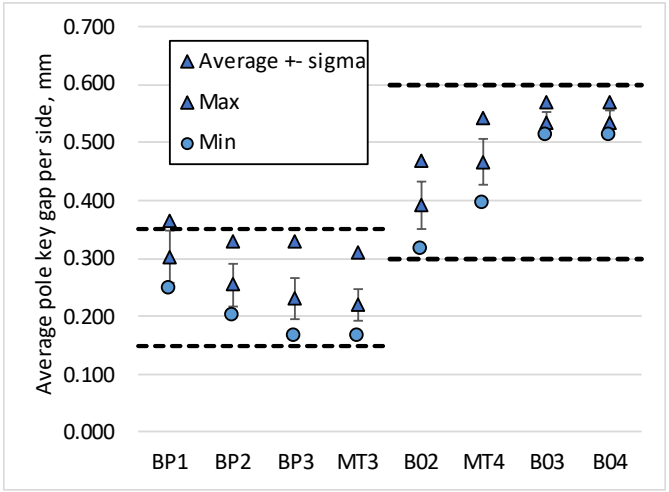

Coil pack geometrical measurements

- For the coil-pack size, uniformity, and squareness the following ranges are set:
  - **The average vertical and horizontal dimension of the coil pack along the z axis shall be within 318.75 mm ± 0.250 mm**
  - **The uniformity of the vertical and horizontal dimensions along the z axis shall be within ±0.200 mm**
  - **The squareness of the vertical and horizontal dimensions along the z axis shall be within±0.250 mm**

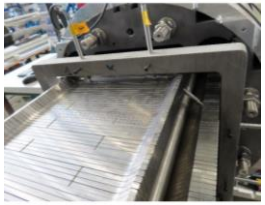

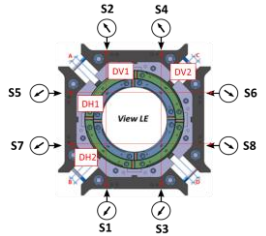

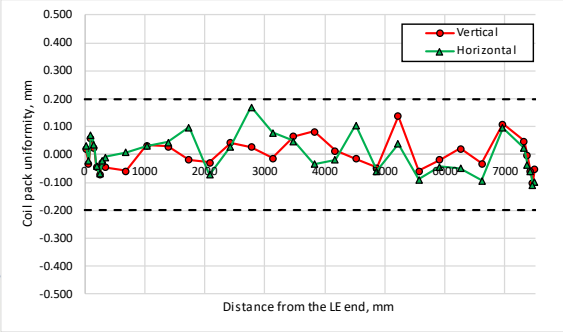

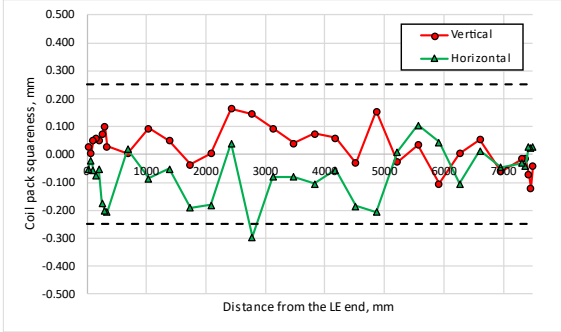

Coil pack size

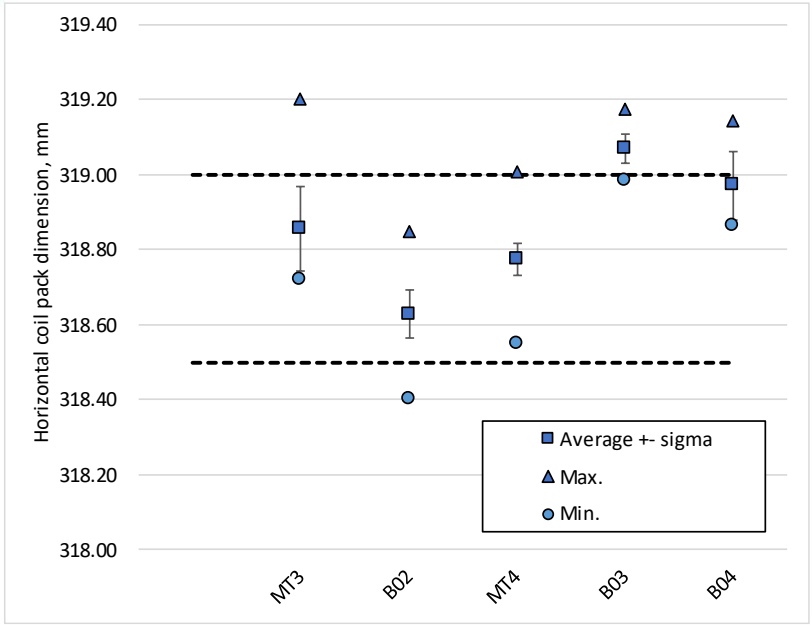

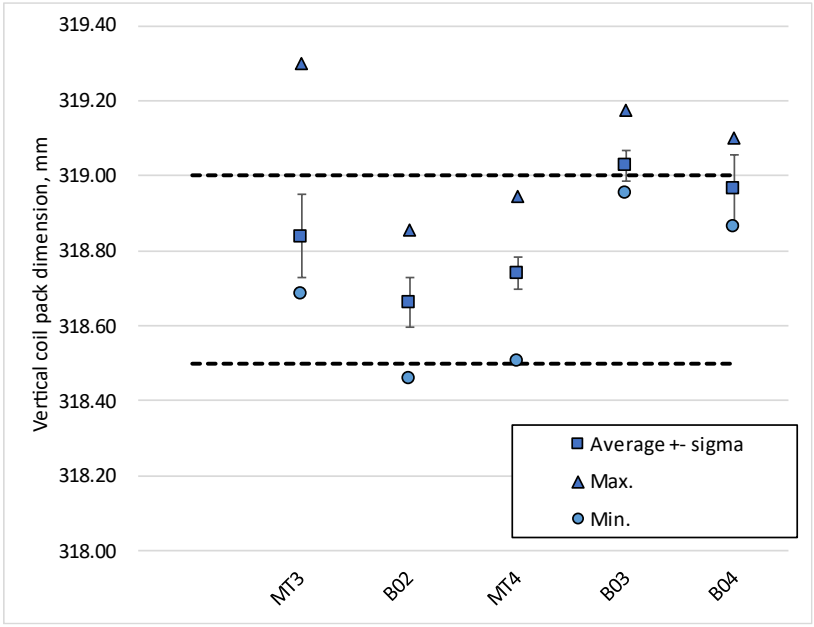

Coil pack squareness and uniformity

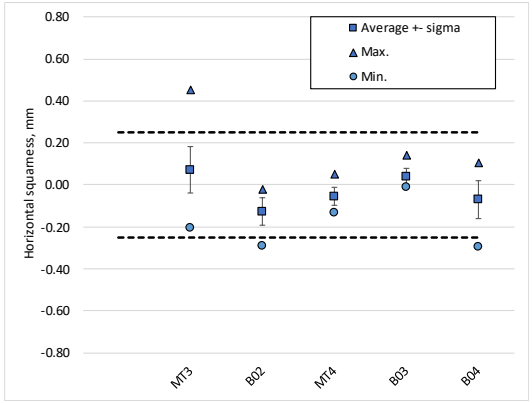

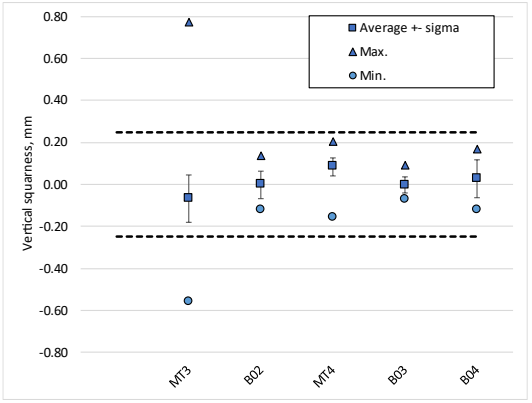

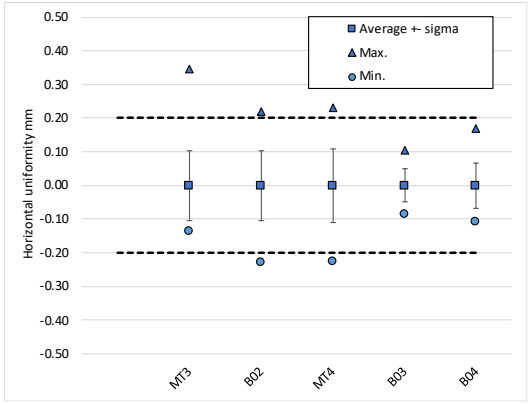

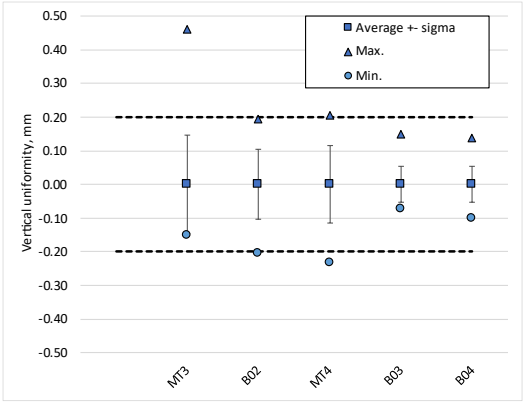

Azimuthal pre-load target

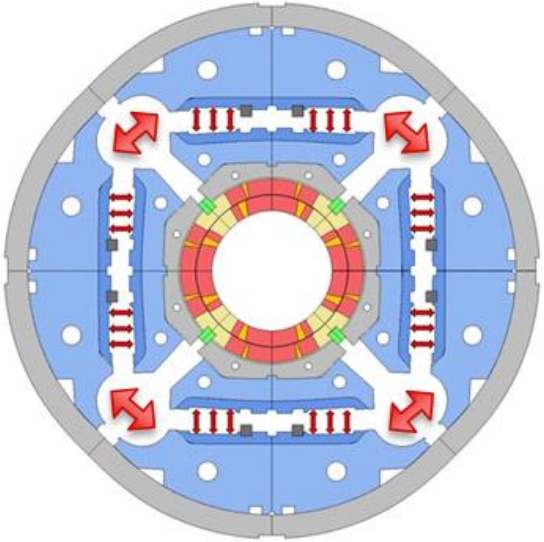

- The allowable peak stress in the coil during loading is -100 MPa, achievable thanks to the new loading procedure with auxiliary bladders.
  - This is a requirement, the measured pole stress in the coils shall not exceed this value
  - The measuring location corresponds to the longitudinal position where we expect higher coil stress (see slide 4)

- The target room temperature preload for MQXFB02 & B03:
  - Average shell stress: 58 ± 6 MPa;
  - Average pole coil stress: -70 ± 10 MPa
  - Rod strain: 650 με
  - This is a target not a requirement, and in case the maximum allowable peak stress in the conductor (100 MPa) is reached, the average pre-load will be lowered accordingly to fulfill the peak stress requirement

- With the new welding procedure, demonstrated in MQXFBP3&B02&B03, we expect no increase on the azimuthal stress of the coils during welding

RT: Targets vs achieved

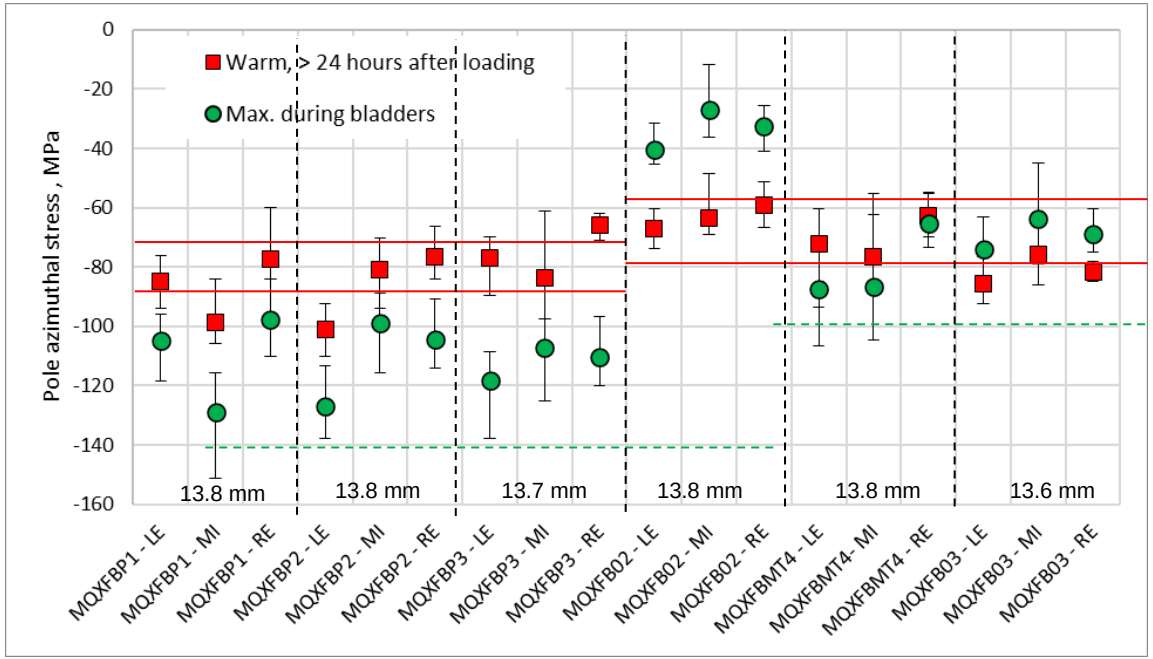

RT: Targets vs achieved

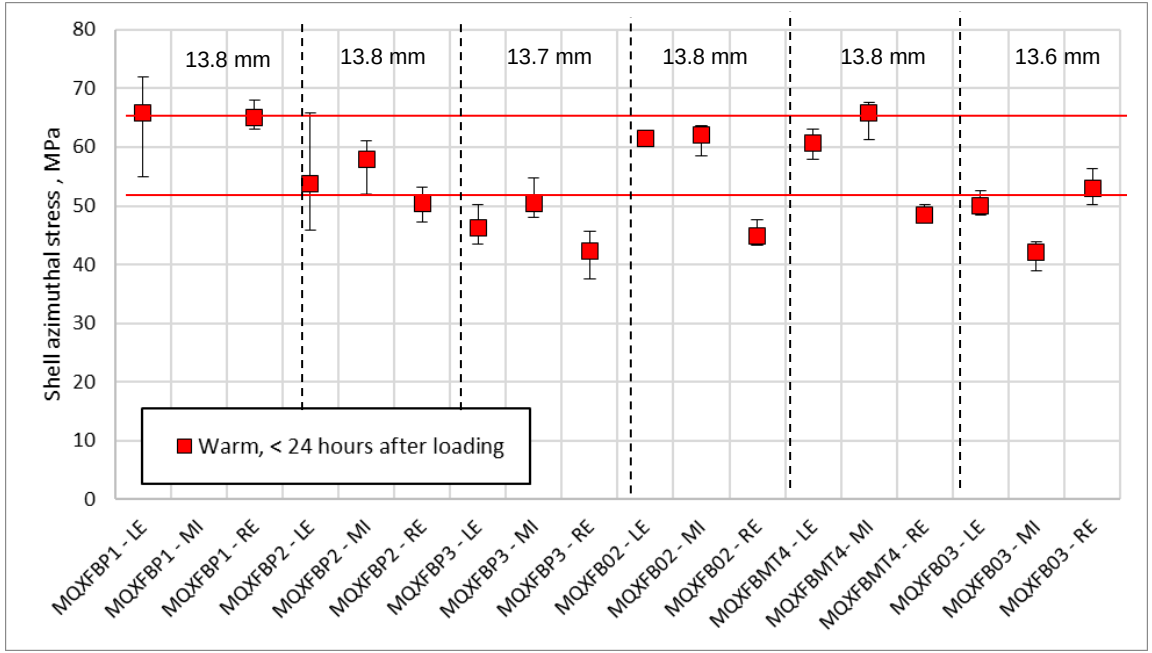

RT transfer function

- So far, relatively good agreement between expected transfer function and measured transfer function
  - In B02/MT4 we show the change of slope due to the new loading procedure
  - In B03 we are closer to the original slope due to the 'new coil geometry'

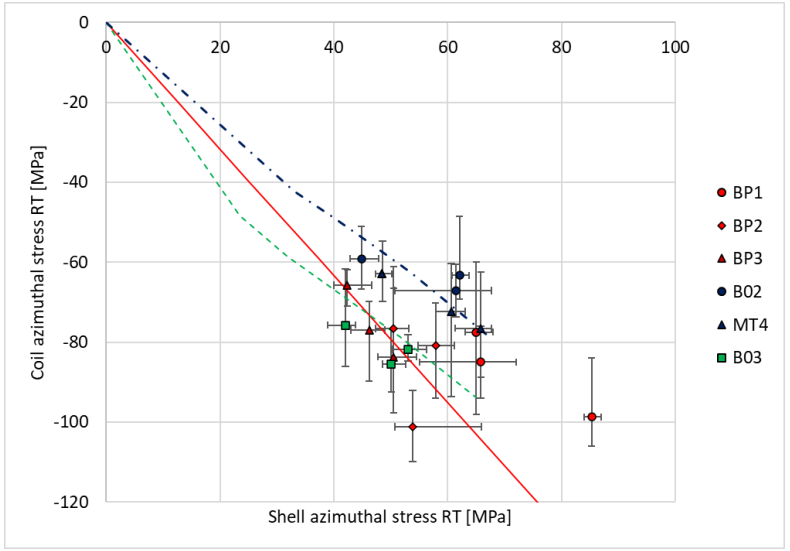

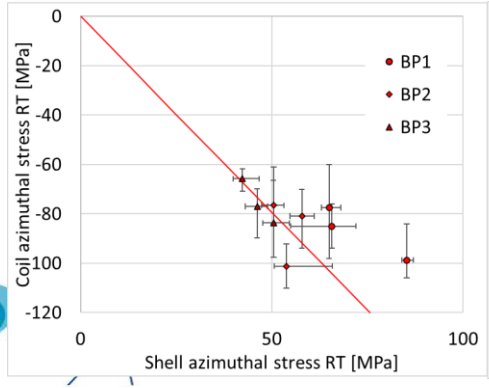

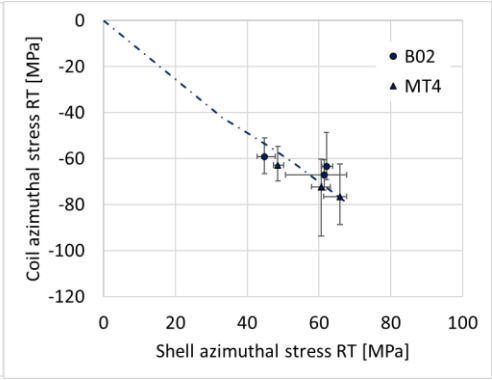

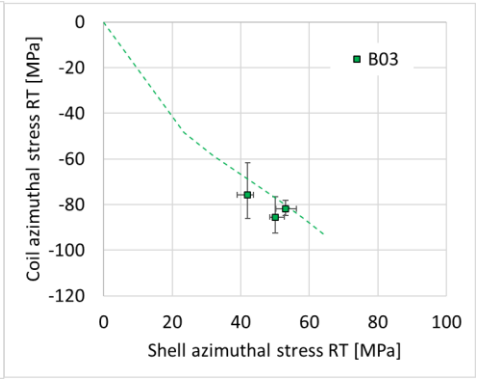

Cold: Targets vs achieved

- At cold, MQXFB02 had 90-110 MPa pole azimuthal compression, corresponding to a pole un-loading around nominal current
- For MQXFB03, we only have ‘clean’ measurements from the LE end, 85 MPa.

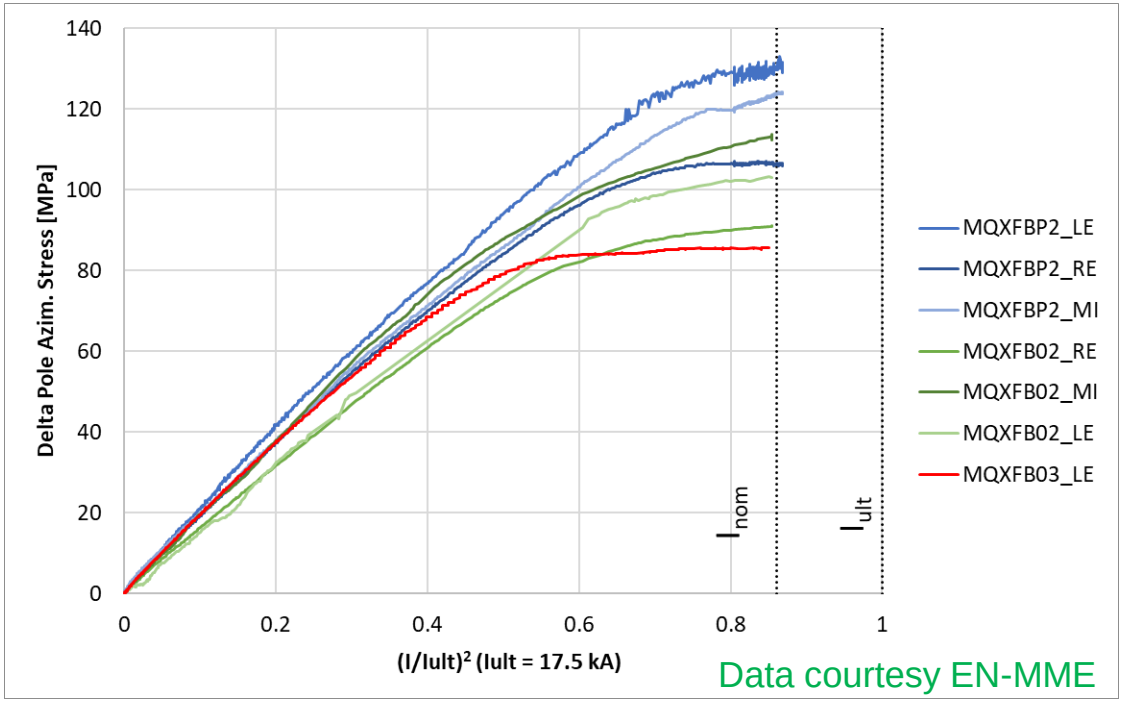

Data courtesy EN-MME

Bladder pressure

- The other observable we have during assembly is the bladder pressure
  - Assembly tolerances play a role, on some occasions, you need 20-30 bars to overcome a singularity in the structure
  - Requirement: never exceed 400 bars

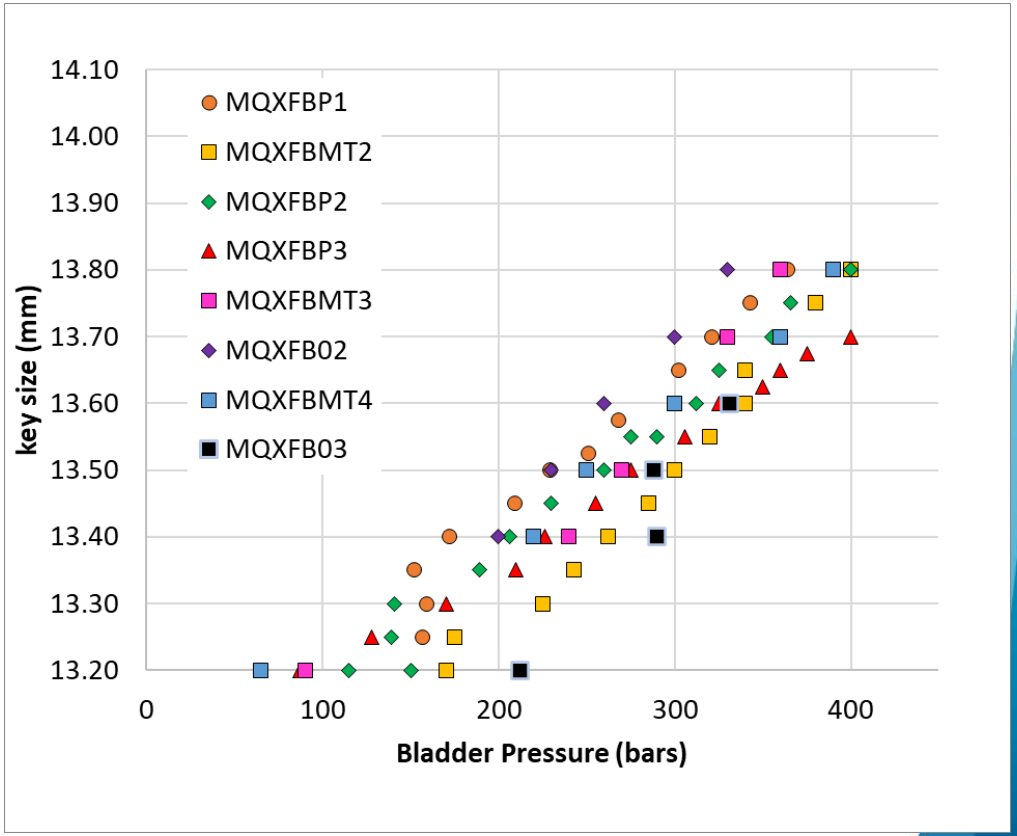

Axial pre-load

- From BP2, all magnets loaded so far with the same axial pre-load (650 ueps at warm)
- Small change of strain on the rods during powering → longitudinal stiffness of the structure is as expected, and overall behaviour is like what we have seen in MQXFS and MQXFA
- MQXFB03 has similar behaviour to the previous magnets, although now the magnet is mostly quenching in the ends

Delta rods strain during powering MQXFB03

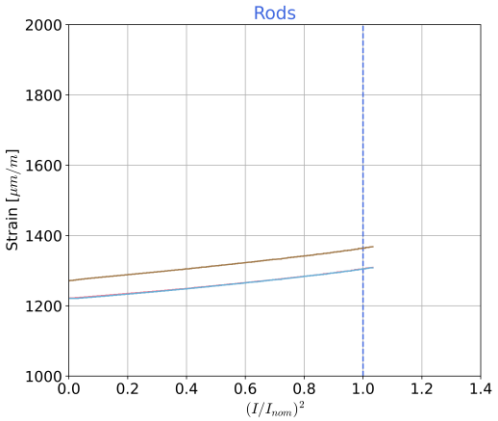

		Δ Rod Strain CD FEM [με]	Δ Rod Strain 16.23 kA FEM [με]	Δ Rod Strain CD [με]	Δ Rod Strain 16.23 kA [με]
Magnet	MQXFBP1	670	35	452	70
	MQXFBP2			461	55
	MQXFBP3			517	75
	MQXFB02			537	75
	MQXFB03			560	85

Azimuthal coil size variation along the length

- Coil geometry significantly changed with the new coil fabrication procedure
- Since we shim to the average coil size (excluding ends), 'new coils' result in magnets with higher pre-load in the ends → more radial friction
  - We don't plan to address this difference with any measure (AUP has concerns on radial pre-load in the ends, so a priori with the new coil geometry we go in the good direction)

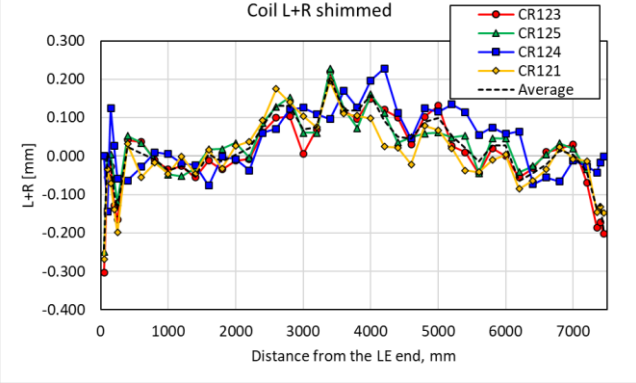

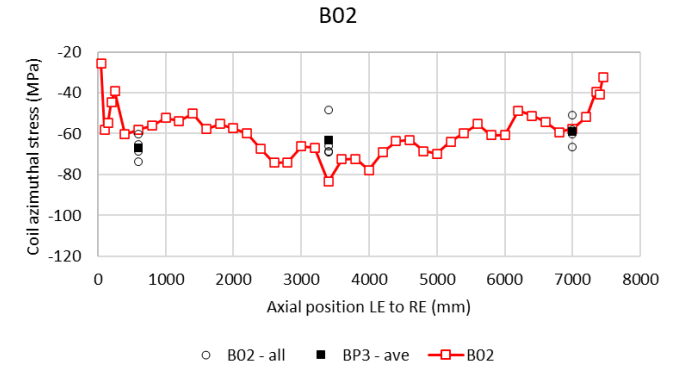

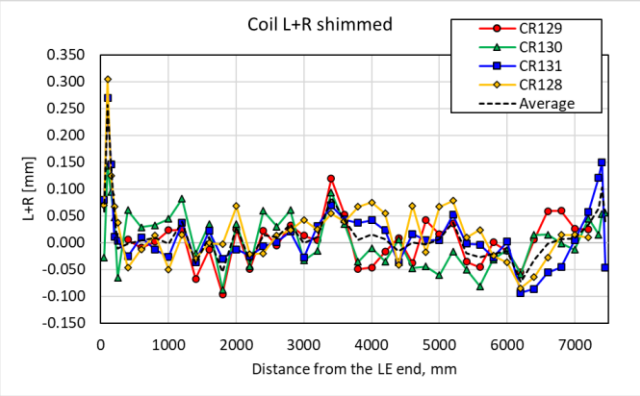

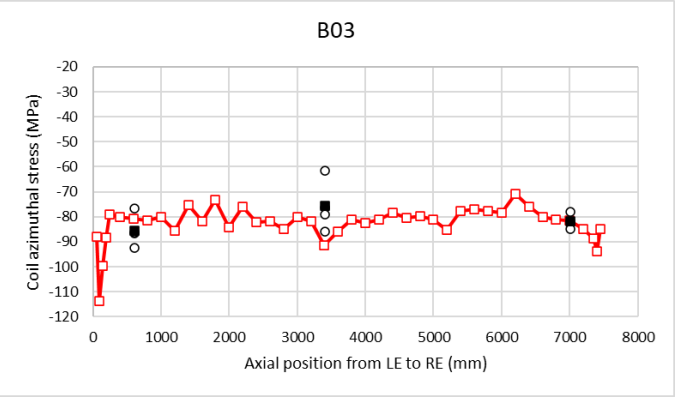

Outline

- Magnets overview
- Lessons learnt
- Overview on assembly data
- **Conclusion**

Conclusions

- The assembly of MQXFB magnets is well mastered, still, minor improvements have been implemented in recent magnets
- In depth analysis of the possible impact of the new generation coil geometry, concluding that non-specific measures had to be taken at the assembly level to accommodate the new coils.
- A detailed set of systematic measurements are performed during assembly, to intercept errors. They will also the base to assess the level of precision we can reach with this type of technology.


Large Magnet Facility
Lenovo

Additional slides

Coil end region B02 vs B03

- The first measuring point is in the heater connection box, due to the presence of resin is a bit smaller than nominal
- The second measuring point is in the metal part of the splice block, nominal dimension
- And then slowly we are going to the coil dimension,
  - for coils with binder in the OL, the coil is bigger than nominal → splice block sees 'lower stress' than the middle of the coil
  - for coils without binder in the OL, the coil is smaller than nominal → splice block sees 'higher stress' than the middle of the coil